The effects of compression loading on perforated cold-formed thin-walled steel structural members of lipped-channel cross-section

MacDonald, Martin; Kotelko, Maria; Kulatunga, Muditha Praveena

Published in:
Proceedings of the 15th Stability of Structures Symposium

DOI:
10.1063/1.5086138

Publication date:
2019

Document Version
Author accepted manuscript

The effects of compression loading on perforated cold-formed thin-walled steel structural members of lipped-channel cross-section

M. Macdonald[1, b)], M. Kulatunga[1], M. Kotełko[2, a)]

[1]*School of Computing, Engineering & Built Environment , Glasgow Caledonian University Glasgow, UK*
[2]*Department of Strength of Materials, Łódź University of Technology, Łódź, Poland*

[a)]maria.kotelko@p.lodz.pl
[b)]M.Macdonald@gcu.ac.uk

Abstract. The effects of perforation position on the compressive load carrying capacity of cold-formed lipped channel sections are studied and discussed. Cold-formed steel sections have become competitive structural components in the modern building construction due to their inherent favourable characteristics over conventional hot-rolled steel members. However, the advantages of these members are often limited due to the presence of perforations. Due to the position of perforations, ultimate strength and elastic stiffness of a structural member can be varied. This paper describes the ultimate strength results obtained from numerical, theoretical and experimental investigations for fixed-fixed end condition. The numerical results were compared with the findings from the experimental investigation results, showed good correlation both with ultimate strength and failure modes. The study showed that the reduction in the stiffness associated with the specimen with perforations on the web was found to be lower than that for the specimen with perforations on the flanges.

INTRODUCTION

Cold-formed steel sections are widely used in building structures, storage racks, transportation machinery, and others. The uses of these products are many and varied. Cold-formed steel sections have a very high strength-to-weight ratio compared with conventional thicker hot-rolled sections. Cold formed steel exhibits a versatile nature which allows for the forming of a range of widely different products, with a variety of shapes, sizes, and applications (Brockenbrough 2009; Cristopher and Schafer 2008; Kulatunga and Macdonald 2012; Kulatunga, Macdonald, Harrison, and Rhodes 2014; Macdonald 2002; Yu 2000). Perforations are used in many cold-formed thin-walled applications to accommodate services such as electrical, plumbing, and heating. Figure 1 shows some of the common perforation shapes used in cold-formed sections.

There are a number of, but not many, research projects that have been conducted on the analyses of cold-formed thin-walled channel section columns with perforations subjected to compression loading. Based on the outcome of the literature review, it can be said that the buckling strength of a structure under compression is largely dependent on the presence/absence of perforations (Macdonald, Heiyantuduwa, Kotelko and Rhodes 2011; Moen and Schafer 2011; Rhodes 1991; Shanmugum, Liew and Thevendran 1998; Yao and Rasmussen 2012). Furthermore, buckling behaviour of compression members with perforations has become a research area of great interest. However, reliable design specifications to predict the ultimate buckling strength of perforated steel sections are

not yet available. The main objectives of this study were to investigate the effects that the position of perforations have on buckling behaviour of cold-formed steel structures and also to attempt to compare these effects using numerical, experimental, and theoretical investigations, and conclusions will be drawn on this basis.

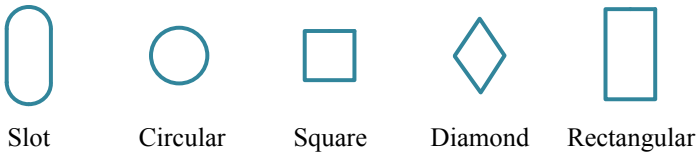

FIGURE 1. Common perforation shapes used in cold-formed sections

NUMERICAL INVESTIGATION

A set of ANSYS modelling guidelines is formalised in this section. Finite element analysis (FEA) is an accurate and flexible technique, which can be used to predict the performance of a structure, mechanism or process under different loading conditions. The non-linear buckling analysis was used to study the buckling behaviour of cold-formed lipped channel sections as detailed in Figure 2.

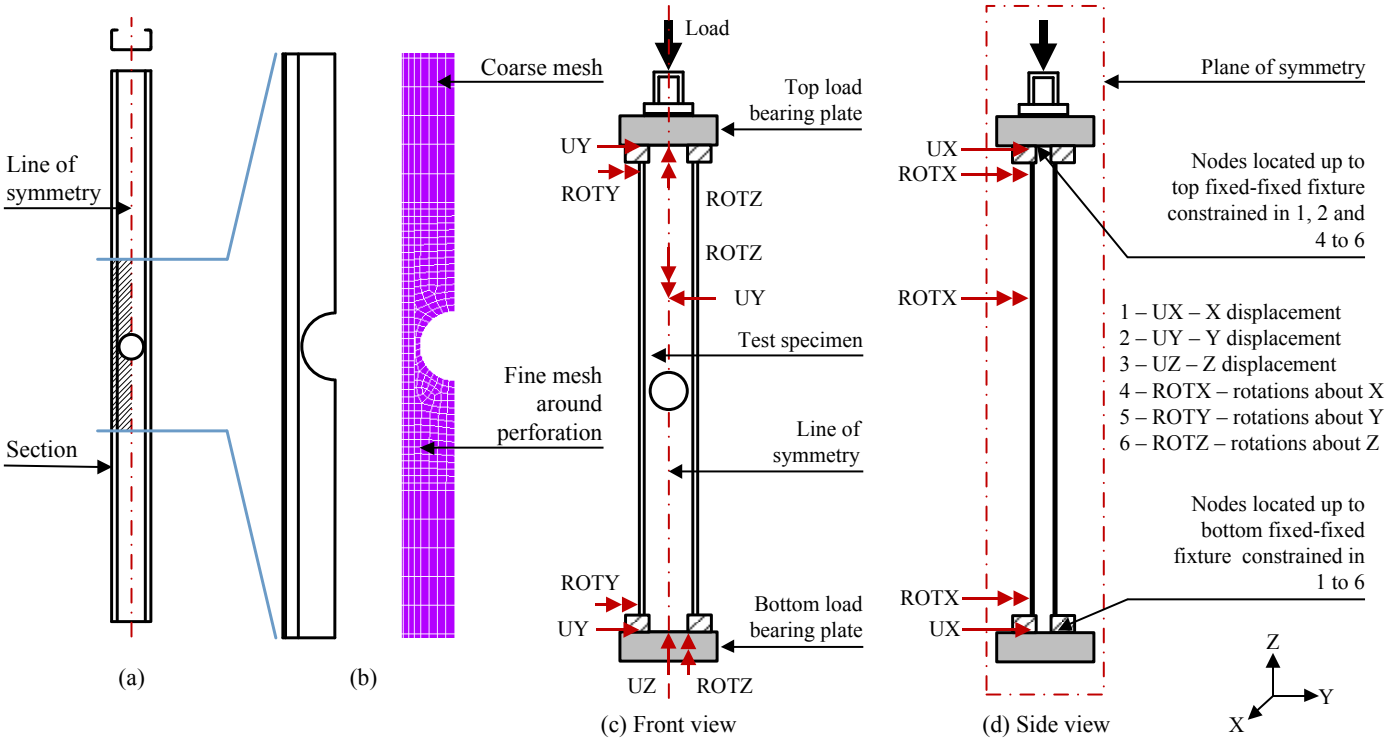

FIGURE 2. [a] Symmetry boundary, [b] mesh type, illustrating different regions of element mesh and [c & d] boundary conditions for fixed-fixed condition

The sections, support reactions and loading were symmetrical about the vertical plane as shown in Figure 2 (a), therefore only one-half of the section was modelled. ANSYS element type SHELL181 was used as it is well-suited for linear, large rotation, and/or large strain nonlinear applications. Load was applied through a load bearing plate which represents the actual loading conditions applied in the experiments. ANSYS element type SOLID45 was used to model the load bearing plates (ANSYS 2010; Hutton 2004;

Kulatunga and Macdonald 2013). An adequate mesh density on contact surfaces and the section was provided, using fine mesh around perforations and coarse mesh further away from the perforations to allow stresses to be distributed in a smooth fashion. Fixed-fixed boundary condition was applied for all loading cases. The symmetric boundary conditions were applied at the symmetry line of the half section. One end of the column was restricted for three degree of freedoms and other end was restricted for two degree of freedoms. Hence, the nodes at the loaded edge of the column have free displacement along the Z direction, but zero displacements along X and Y directions and zero rotations about X, Y and Z axes. The bottom edge of the column was assumed to have zero displacements along X, Y, and Z directions and zero rotations about X, Y and Z axes as shown in Figures 2 (c) and (d).

ANALYTICAL INVESTIGATION – YIELD LINE ANALYSIS

An alternative method to predict an ultimate load , using the algorithm based on Yield Line Analysis (YLA) of the plastic mechanism of failure was also applied (Kotełko, 2004,2010). The method enables the estimation of the ultimate load at the intersection point of the pre-buckling path and post-failure curve (evaluated on the basis of YLA). Two basic plastic mechanisms were applied to evaluate post-failure curves, namely three-hinge flange mechanism and pitched-roof mechanism (Ungureanu et al. 2010). The main advantage of this method is the simplicity of the applied algorithm and a very short time of calculation, competitive with FE calculations. The perforations were taken into account using reduction factors of fully plastic moments (Kotełko, 20101) at certain yield lines of the plastic mechanism.

EXPERIMENTAL INVESTIGATION

Cold-formed steel lipped channel sections with perforations were tested to failure. A test programme was carried out on lipped channel sections with fixed-fixed boundary conditions. Experimental results were reported and used to validate finite element analysis results. Table 1 illustrates the column testing parameters and material properties employed in this research work. Two sets of identical clamping attachments were manufactured as shown in Figure 3 to achieve fixed-fixed end conditions.

Table 1: Column testing parameters and material properties.

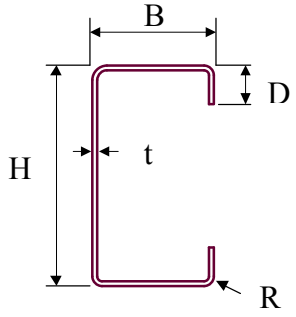

Cross-section	
H (mm)	120.00
B (mm)	50.00
D (mm)	15.00
R (mm)	3.00
t (mm)	1.15
Average yield strength, σ_y (N/mm^2)	195
Modulus of elasticity, E (N/mm^2)	210500

Set 1

In this study, a set of experiments was carried out to study the influence of a perforation area on the buckling strength of column members. The specimens were selected to have same cross-section dimensions, but with different perforation areas as shown in Figure 4. The column lengths were kept constant. The columns were tested with fixed-fixed end conditions. The column testing parameters are listed in Table 2.

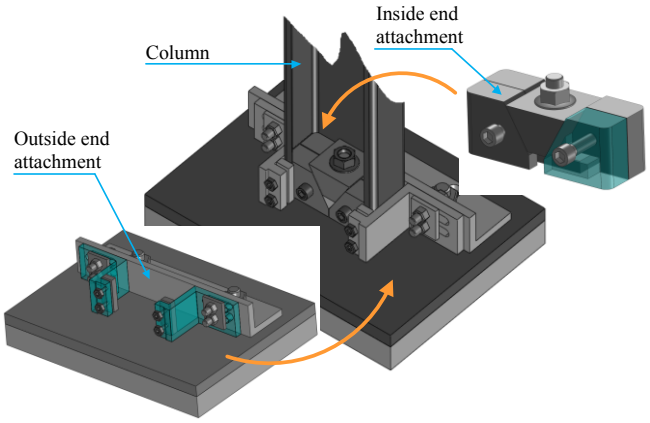

FIGURE 3. Fixed-fixed end attachment, holding a column member into a fixed position.

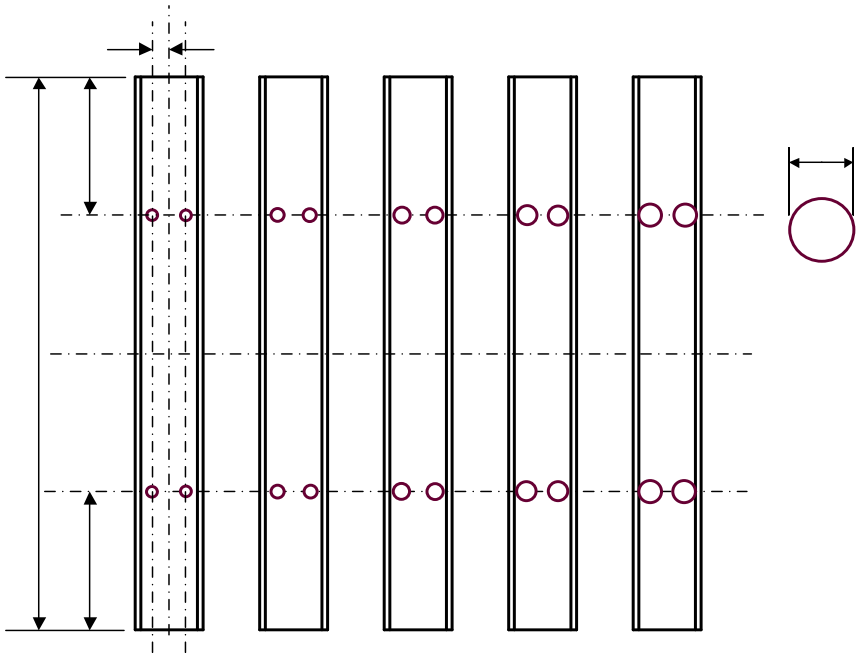

FIGURE 4. Perforation shapes and positions – Set 1.

Set 2

In Set 2, a range of specimens of the same cross-section but with different perforation areas was tested to failure. In this investigation, column lengths and cross-section dimensions were kept constant, with perforations located on flanges of the columns as shown in Figure 5. The columns were tested with fixed-fixed end conditions. Table 3 shows the column testing parameters.

Table 2: Nominal section dimensions – Set 1.

Specimen		Length of the specimen	Ø $_{perforation}$	W_1
1-1	SIII/S1-1/P/F-F	L	3 b	c
1-2	SIII/S1-2/P/F-F	L	4 b	c
1-3	SIII/S1-3/P/F-F	L	5 b	c
1-4	SIII/S1-4/P/F-F	L	6 b	c
1-5	SIII/S1-5/P/F-F	L	7 b	c
			L = 1000 mm, b = 5 mm, c = 30 mm	

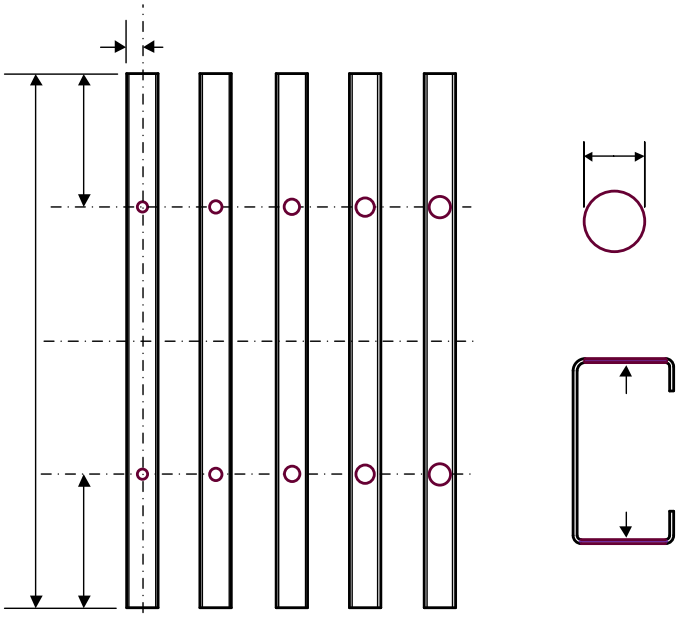

FIGURE 5: Perforation shapes and positions – Set 2.

Table 3: Nominal section dimensions – Set 2.

Specimen		Length of the specimen	Ø $_{perforation}$	W_2
2-1	SIII/S2-1/P/F-F	L	3 b	c
2-2	SIII/S2-2/P/F-F	L	4 b	c
2-3	SIII/S2-3/P/F-F	L	5 b	c
2-4	SIII/S2-4/P/F-F	L	6 b	c
2-5	SIII/S2-5/P/F-F	L	7 b	c
			L = 1000 mm, b = 5 mm, c = 25mm	

OBSERVATIONS

Set 1

In this study, flanges started to buckle by deflecting in an outward direction when the load reached around 85% of the ultimate load. All the specimens failed by local buckling mixed with distortional buckling at the peak load forming three distortional buckling half-waves. Maximum deformation occurred around the perforations near to the bottom end in the specimens 1-2 to 1-4 whereas, in specimens 1-1 and 1-5, the maximum deformation occurred around the perforations near to the top end.
According to the above observations, a typical flange mechanism (Fig. 6a) was observed at the post-ultimate stage.

It was observed that the reduction in stiffness increased with the increase in the diameter of perforations. The experimental percentage reduction in the ultimate load for the specimen with higher and lower reduction in the stiffness is 7.69%.

Set 2

The comparisons of results show that, the ultimate load of the specimen under compression varies with the size of the perforation. It was observed that the ultimate load decreased with the increase in the diameter of perforations. It was observed during the loading process, the lateral displacement of flanges started to increase in an inward direction and interaction of local and distortional buckling modes were noticed around 80% of the ultimate load. Three distortional buckling half-waves along the flanges were also noticed. The reduction in the stiffness associated with specimens 2-1 to 2-5 was found to be around the perforations near to the bottom end. The difference between the experimental higher and lower ultimate load values is 18.41%. In this case, a web mechanism (Fig. 6b) , identified as a pitched-roof mechanism was observed in the post-ultimate stage.

Comparisons of Theoretical Results with Experimental Results

Finite element models that incorporate the column testing parameters described in the experimental investigation were compared with test results for the purpose of investigating the buckling behaviour and ultimate strength of cold-formed steel members with perforations. The comparisons of numerical and experimental are shown in Figure 6 for Sets 1 and 2.

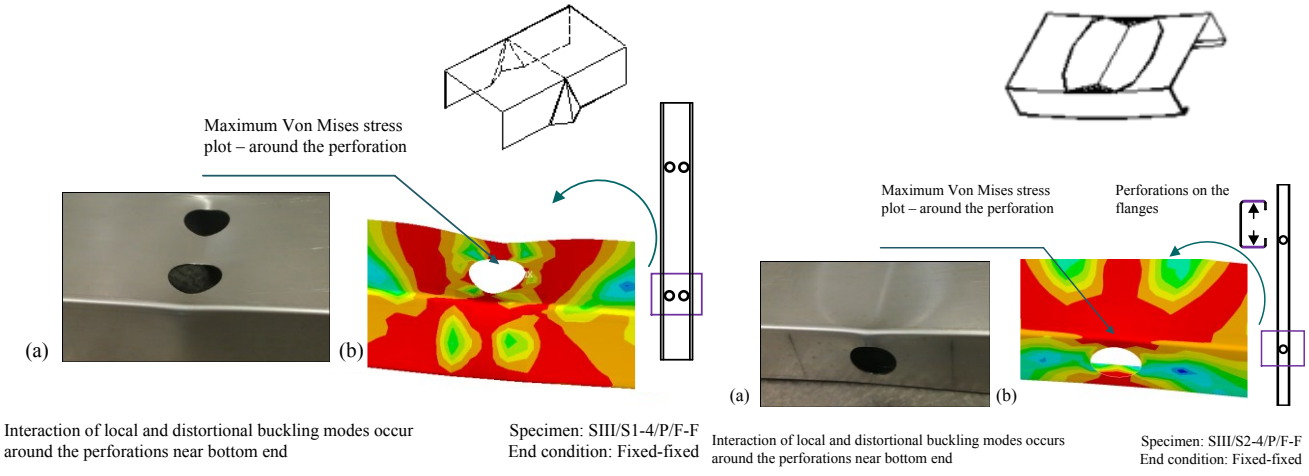

FIGURE 6: Comparison of experimental and finite element analysis deformed shape: (a) experimental deformed shape around the perforation and (b) ANSYS deformed shape around the perforation, equivalent half section for the sections SIII/S1-4/P/F-F (1-4) and SIII/S2-4/P/F-F (2-4).

(a)

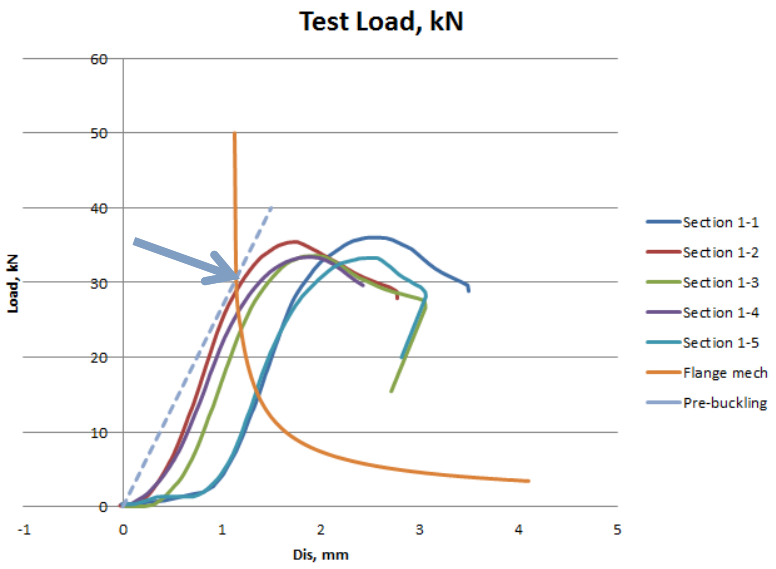

(b)

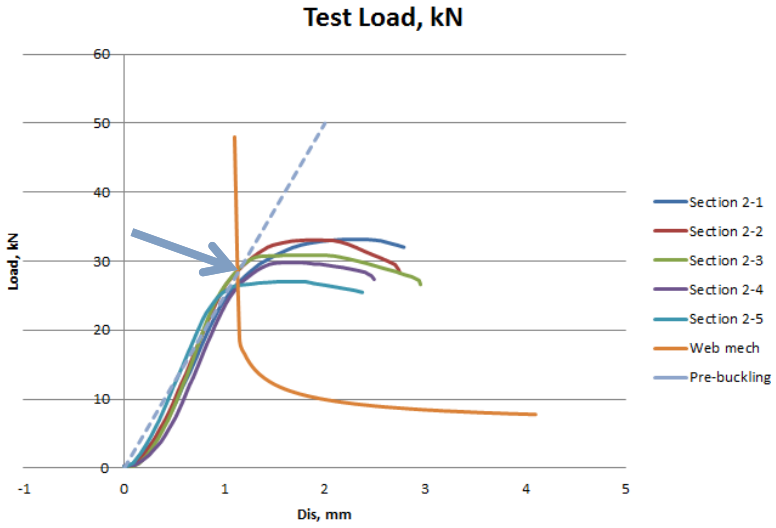

FIGURE 7: Experimental load-shortening diagrams and YLA post-failure curves: a) set 1, b) set 2.

Figure 7 shows the rest of all the experimental load-shortening curves for set 1 and set 2 respectively. On both diagrams, pre-buckling paths together with YLA post-failure curves, corresponding to the highest contribution of perforation (for set 1-5 and 2-5 respectively) are shown. The character of theoretical post-failure curves was similar to post-ultimate sections of experimental curves, although tests stopped before plastic mechanisms were entirely developed.

Comparisons of Numerical Results and Design Code Predictions with Experimental Results

The comparisons of numerical results and design code predictions computed from AISI Specifications (2012), British Standards - BS 5950 Part 5 (1998), and Eurocode 3 - ENV 1993-1-3:2009 (2009) with experimental results are shown in Table 4. It was noticed from the literature that the design code recommendations were largely based on ultimate load, and hence, only ultimate buckling loads are used in the comparisons. Ultimate buckling load can be noted accurately using load vs. displacement graph. The comparisons were mainly carried out using load vs. displacement graphs.

Table 4: Comparisons of numerical results and design code predictions with experimental results.

	Specimen		Ultimate Buckling Strength (kN)					Ultimate Load Ratio			
			Test, $P_{exp, U}$	FEA $P_{FEA, U}$	AISI, P_{cre}	BS 5950, $P`_c$	Eurocode, $N_{b,Rd}$	$P_{FEA, U}$ / $P_{exp, U}$	P_{cre} / $P_{exp, U}$	$P`_c$ / $P_{exp, U}$	$N_{b,Rd}$ / $P_{exp, U}$
Set 1	1-1	SIII/S1-1/P/F-F	36.03	35.70	39.53*	36.36	40.14	0.99	1.10*	1.01	1.11
	1-2	SIII/S1-2/P/F-F	35.42	38.52	38.56*	35.22	39.04	1.09	1.09*	0.99	1.10
	1-3	SIII/S1-3/P/F-F	33.56	33.99	38.07*	34.26	38.55	1.01	1.13*	1.02	1.15
	1-4	SIII/S1-4/P/F-F	33.40	32.63	37.88*	33.20	38.65	0.98	1.13*	0.99	1.16
	1-5	SIII/S1-5/P/F-F	33.26	32.53	36.51*	31.12	38.13	0.98	1.10*	0.94	1.15
		30.05**					Mean, $\overline{X}$	1.01	1.11	0.99	1.13
							Standard Deviation, S	0.05	0.02	0.03	0.02
							Coefficient of Variation, COV	0.05	0.02	0.03	0.02
Set 2	2-1	SIII/S2-1/P/F-F	33.14	33.50	32.43*	30.00	33.41	1.01	0.98*	0.91	1.01
	2-2	SIII/S2-2/P/F-F	33.05	32.30	30.33*	28.35	31.46	0.98	0.92*	0.86	0.95
	2-3	SIII/S2-3/P/F-F	30.87	30.10	27.77*	26.33	28.99	0.98	0.90*	0.85	0.94
	2-4	SIII/S2-4/P/F-F	29.78	28.60	26.19*	24.66	27.48	0.96	0.88*	0.83	0.92
	2-5	SIII/S2-5/P/F-F	27.04	26.31	23.79*	22.23	25.13	0.97	0.88*	0.82	0.93
		28.95**					Mean, $\overline{X}$	0.98	0.91	0.85	0.95
							Standard Deviation, S	0.02	0.04	0.03	0.03
							Coefficient of Variation, COV	0.02	0.04	0.04	0.04

* *Section/perforation dimensions do not comply with AISI specification,* ** *YLA ultimate load prediction for set 1-5 and 2-5*

CONCLUSIONS

The comparisons between the test results in Set 1 and Set 2 pointed out, that the reduction in the stiffness associated with the specimen with perforations on the web was found to be lower than that for the specimen with perforations on the flanges. The experimental and numerical investigations showed that in the case of slender cross-sections, which are substantially affected by local buckling and distortional buckling, the movement of the flanges generally follow an outward direction and showed three distortional half-waves at the peak load in many cases. Interaction of local and distortional buckling modes was observed adjacent to the perforations in all specimens at the failure load.

It was shown that numerical and experimental investigations can be used to obtain a better understanding of failure mechanisms of buckling in lipped channel sections with perforations with a reasonable degree of confidence. Further, the investigation showed that the ultimate load of the structure under compression varied greatly with the position of perforations. Moreover, the results also indicated that current design rules in American Iron and Steel Institute (AISI), British Standards (BS), and European Recommendations are conservative for the load capacity of column members of lipped channel cross-section with perforations subjected to compression loading.

YLA curves (at intersection with pre-buckling path) give conservative predictions of ultimate load. However, for some cases the predictions were less conservative than those of the design standards.

REFERENCES

1. American Iron and Steel Institute., 2012, North American Cold-Formed Steel Specification for the Design of Cold-Formed Steel Structural Member.
2. ANSYS., 2010. ANSYS Mechanical APDL Structural Analysis Guide: ANSYS Release 13.0. USA.
3. British Standards Institution, BS5950., 1998, British Standards for Structural Use of Steel Work in Buildings – Part 5: Code of Practice for Design of Cold Formed Thin Gauge Sections.
4. Brockenbrough, R.L., 2009, *Highway Engineering Handbook*. 3rd ed. USA: McGraw-Hill Companies, Inc. ISBN 978-0-07-159763-0.
5. Cristopher, D.M. and Schafer, B.W., 2008, Experiments on Cold-Formed Steel Columns with Holes. Thin-Walled Structures Vol. 46(10), pp 1164-1182.
6. ENV 1993-1-3:2006, Eurocode 3., 2009, Design of Steel Structures; Part 1.3: General Rules - Supplementary Rules for Cold Formed Thin Gauge Members and Sheeting.
7. Hutton, D.V., 2004, Fundamentals of Finite Element Analysis. USA: McGraw-Hill Companies, Inc. ISBN 0-07-239536-2.
8. Kulatunga, M. and Macdonald, M., 2012, Investigation of Cold-Formed Steel Structural Members With Perforations of Different Shapes Subjected to Compression Loading, Proceedings of the 6th International Conference on Couple Instabilities in Metal Structures, Glasgow, Scotland, 3-5 December.
9. Kulatunga, M. and Macdonald, M., 2013, Investigation of Cold-Formed Steel Structural Members with Perforations of Different Arrangements Subjected to Compression Loading. Thin-Walled Structures. Vol. 67, pp 78-87, ISSN: 0263-8231.
10. Kulatunga, M., Macdonald, M., Harrison, D. K. and Rhodes, J., 2014, Load Capacity of Cold-Formed Column Members of Lipped Channel Cross-Section with Perforations Subjected to Compression Loading – Part 1: FE Simulation and Test Results. Thin-Walled Structures. Vol. 80, pp 1-12, ISSN: 0263-8231.
11. Kulatunga, M. and Macdonald, M., 2014, The Efficient Design of Cold-Formed Perforated Thin-Walled Steel Structural Member Subjected to Compression Loading, Proceedings of the 7th International Conference on Thin Walled Structures, Busan, South Korea, 28 September – 2 October.
12. Kotelko, M., Lis, P and Macdonald, M., 2014, Load-Capacity Probabilistic Sensitivity Analysis of Thin-Walled Beams, Proceedings of the 7th International Conference on Thin Walled Structures, Busan, South Korea, 28 September – 2 October.
13. Macdonald, M., 2002, The Effects of Cold Forming on Material Properties and Post-Yield Behaviour of Structural Sections. Ph.D. thesis, Glasgow Caledonian University.
14. Macdonald, M., Heiyantuduwa Don, M.A., Kotelko, M. and Rhodes J., 2011, Web Crippling Behaviour of Thin-Walled Lipped Channel Beams. Thin-Walled Structures Vol. 49(5), pp 682-690.
15. Moen, C. and Schafer, B., 2011, Direct Strength Method for Design of Cold-Formed Steel Columns with Holes, J. Struct. Eng, Vol. 137(5), pp 559–570.
16. Rhodes, J., 1991, *Design of Cold-Formed Steel Members.* England: Elsevier Applied Science. ISBN 1-85166-595-1.
17. Shanmugum, N.E., Liew, J.Y.R. and Thevendran, J.Y.R., 1998, Thin-Walled Structures Research and Development Second International Conference on Thin-Walled Structures. Oxford, UK: Elsevier Science Ltd. ISBN: 0-08-043003-1.
18. Yao, O. and Rasmussen, K.J.R., 2012, Inelastic Local Buckling Behaviour of Perforated Plates and Sections Under Compression, Thin-Walled Structures, Vol. 61, pp 49-70.
19. Yu, W.W., 2000, *Cold-Formed Steel Structures.* 3rd ed. Canada: John Wiley & Sons Inc. ISBN 0-471-34809-0.
20. V. Ungureanu, M. Kotełko, R.J. Mania, D. Dubina, "Plastic mechanisms database for thin-walled cold-formed steel members in compression and bending," *Thin-Walled Structures*, 48(10-11), 818-826 (2010).
21. M. Kotełko, 2010. Load-carrying capacity and mechanisms of failure of thin-walled structures (in Polish). WNT Warszawa.